AIAA JOURNAL
Vol. 31, No. 11, November 1993

Mass-Additive Modal Test Method for Verification of Constrained Structural Models

John R. Admire,* Michael L. Tinker,† and Edward W. Ivey‡
NASA Marshall Space Flight Center, Huntsville, Alabama 35812

A method for deriving constrained or fixed-base modes and frequencies from free-free modes of a structure with mass-loaded boundaries is developed. Problems associated with design and development of test fixtures can be avoided with such an approach. The analytical methodology presented is used to assess applicability of the mass-additive method for three types of structures and to determine the accuracy of derived constrained modes and frequencies. Results show that mass loading of the boundaries enables local interface modes to be measured within a desired frequency bandwidth, thus allowing constrained modes to be derived with considerably fewer free-free modes than for unloaded boundaries. Good convergence was obtained for a simple beam and a truss-like Shuttle payload, both of which had well-spaced modes and stiff interface support structures. Slow convergence was obtained for a space station module prototype, a shell-like structure having high modal density.

Nomenclature

$\{f(t)\}$	= external force vector
$[I]$	= identity matrix
$[K]$	= stiffness matrix
$[M]$	= original mass matrix
$[\bar{M}]$	= mass-additive mass matrix
N	= size of original system matrices
n	= number of measured or selected mass-additive modes
n_B	= number of boundary degrees of freedom
$\{q_m\}$, $\{\ddot{q}_m\}$	= mass-additive coordinates
$\{\hat{q}_m\}$, $\{\ddot{\hat{q}}_m\}$	= reduced mass-additive coordinates
$\{\bar{q}_m\}$	= eliminated mass-additive coordinates
$[T_c]$	= transformation to constrain boundaries
$\{x\}$, $\{\ddot{x}\}$	= physical coordinates
$[\Delta M]$	= added mass
$[\hat{\Phi}]$	= modes in reduced coordinates
$[\Phi_m]$	= mass-additive mode shapes
$[\hat{\Phi}_m]$	= partition of mass-additive modes related to reduced coordinates
$[\bar{\Phi}_m]$	= partition of mass-additive modes related to eliminated coordinates
$[\Phi_R]$	= exact constrained mode shapes
$[\bar{\Phi}_R]$	= derived constrained modes
$[\hat{\omega}^2]$	= frequencies in reduced coordinates
$[\omega_m^2]$	= mass-additive frequencies

Subscripts and Superscripts

B	= boundary degrees of freedom
I	= interior degrees of freedom

Introduction

TO develop a verified dynamic mathematical model of a constrained structure, it is necessary to perform a modal survey test of the physical structure and then modify the pretest mathematical model to obtain the best possible agreement with the test data. Constrained-boundary, or fixed-base, modal tests have traditionally been used for improving constrained models, since the measured modes and frequencies can be used directly in the model verification process. However, there are a number of difficulties associated with fixed-base modal testing, in some cases making the approach impractical. First, it is impossible to achieve a truly fixed-base test since the fixture will have some degree of coupling with the test article. The extent of contamination of the test data due to such coupling depends on the number of fixture modes, and the characteristics of those modes, within the frequency bandwidth of the test. Second, the boundary constraints experienced by the structure in service may be extremely difficult to simulate in a constrained test. Undesired motion may occur between the test article and the fixture at connections that are welded, bolted, or constructed using lubricated bearings. The fixture may also impose constraints on the test article that do not exist in service. Finally, the cost of designing and constructing a fixture for constrained tests may be prohibitive.

To provide alternate approaches for verifying constrained models when fixed-base testing proves impractical, several free-boundary modal test techniques have been investigated, including the mass-additive technique.[1] Goldenberg and Shapiro,[2] Gwinn et al.,[3] and Baker[4] consider the use of mass loading for component mode synthesis, whereas the current paper and Refs. 1 and 5 consider the mass-additive method for verification of a constrained model. To this point, use of the mass-additive method has been limited due to the lack of a well-defined theoretical basis to guide design of the boundary masses and establish limitations for the technique. The purpose of this paper is to investigate general applicability of the mass-additive method as an alternative to fixed-base testing by developing a theoretical basis for the technique and using the results of mass-additive tests. In the following sections, the method is described in detail, and the governing equations are derived. The technique is demonstrated for a simple beam, and then for two classes of Space Shuttle payloads.

Description of the Mass-Additive Method

It is well known that for coupled substructures the interfaces must be adequately characterized to allow accurate transient response analysis. This is especially true for Shuttle payloads that are constrained at a number of discrete points (Fig. 1). The dynamic response of the payload is largely controlled by the stiffnesses of the interfaces (trunnions and keel). For this reason, one of the primary objectives of modal testing

Received June 9, 1992; revision received April 13, 1993; accepted for publication April 13, 1993.

*Technical Assistant, Structural Analysis Division.
†Aerospace Technologist, Payload Dynamics and Loads Branch, Structural Analysis Division.
‡Chief, Payload Dynamics and Loads Branch, Structural Analysis Division.

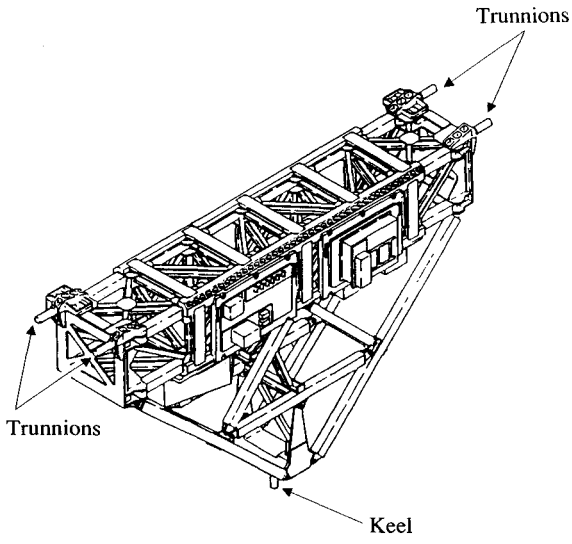

Fig. 1 Shuttle payload with Orbiter connections.

of Shuttle payloads is to measure interface characteristics so that the mathematical model can be refined at the interfaces.

Obviously, a constrained-boundary test allows direct measurement of the modes that are controlled by the interfaces. However, in a free-boundary support configuration the interface modes occur at higher frequencies than the structure global modes. This increases the time required to measure both the local interface modes and the global modes in one test due to the large frequency bandwidth required. Furthermore, it is difficult to develop a mathematical model with fidelity over a large frequency range. A model that accurately represents low-frequency global modes may require extensive refinement to reliably predict localized high frequency modes.[6]

In the mass-additive technique, the boundaries are mass loaded to lower the frequencies of the interface modes and to bring the modes into the frequency bandwidth of the global modes. The idea of attaching masses to structure boundary degrees of freedom in modal testing is similar to the concept presented by Benfield and Hruda[7] for modal synthesis. A typical Shuttle payload with mass-loaded boundaries is shown in Fig. 2. In addition to narrowing the frequency bandwidth, the added masses also allow the interfaces to be exercised to a greater degree than is possible in a usual free-boundary configuration. Interface modes are obtained due to extensive excitation of the structure in the interface regions. From a modeling standpoint, the added masses are easily included as rigid bodies having known mass and inertia attached to the boundary degrees of freedom.

Modal testing using boundary masses has been successfully performed (Refs. 1, 5, and 8) and the test data used to improve mathematical models. However, an analytical treatment of the technique is required to assess the limits of applicability, to provide guidelines for design of the boundary masses, and to determine the number of mass-additive test modes needed for deriving accurate constrained modes. The governing equations for deriving constrained modes and frequencies from a mass loaded free-boundary structural configuration are derived in the next section.

Formulation of Constrained Equations of Motion in Terms of Mass-Additive Modes

In a free-boundary mass-additive modal test, masses are attached to the interface degrees of freedom as shown in Fig. 2. The undamped equations of motion for a test article in this configuration can be written as

$$[\bar{M}]\{\ddot{x}\} + [K]\{x\} = \{f(t)\} \tag{1}$$

where $[\bar{M}] = [M] + [\Delta M]$ and $[\Delta M]$ represents the mass added to the boundaries. Using the mode shapes obtained in the solution of Eq. (1), the displacements are

$$\{x\} = [\Phi_m]\{q_m\} \tag{2}$$

where $[\Phi_m]$ represents the measured mass-added modes in a test application. These modes can also be generated analytically using a mass-loaded finite element model that has been tuned or improved using measured mass-additive modes. The latter approach is taken in this paper. Transformation of Eq. (1) using Eq. (2) yields the mass-additive equations of motion in generalized form,

$$[\Phi_m]^T[\bar{M}][\Phi_m]\{\ddot{q}_m\} + [\Phi_m]^T[K][\Phi_m]\{q_m\} = [\Phi_m]^T\{f(t)\} \tag{3}$$

where the mode shape matrix is $N \times n$. The mass-added coordinates obtained from a solution of Eq. (3) allow the calculation of the physical displacements by using Eq. (2).

To derive constrained modes from a free-free mass-added model, it is necessary to express the equations of motion of the model with unloaded boundaries in terms of mass-additive mode shapes. This is done by subtracting the $[\Delta M]$ term from Eq. (3), yielding

$$(I - [\Phi_m]^T[\Delta M][\Phi_m])\{\ddot{q}_m\} + [\omega_m^2]\{q_m\} = [\Phi_m]^T\{f(t)\} \tag{4}$$

where $[I] = [\Phi_m]^T[\bar{M}][\Phi_m]$ and $[\omega_m^2] = [\Phi_m]^T[K][\Phi_m]$. Separating the original coordinates in Eq. (2) into interior and boundary degrees of freedom yields the expression

$$\{x\} = \begin{Bmatrix} x_I \\ x_B \end{Bmatrix} = [\Phi_m][q_m] \tag{5}$$

and if the mass-added modal matrix and generalized coordinates are separated in the same manner,

$$\begin{Bmatrix} x_I \\ x_B \end{Bmatrix} = \left[\begin{array}{c|c} \bar{\Phi}_m^I & \hat{\Phi}_m^I \\ \hline \bar{\Phi}_m^B & \hat{\Phi}_m^B \end{array}\right] \begin{Bmatrix} \bar{q}_m \\ \hat{q}_m \end{Bmatrix} \tag{6}$$

The generalized coordinates $\hat{q}_m$ represent a reduced set of mass-added vectors that is smaller than the measured or retained analytical set by n_B, the number of boundary degrees of freedom. Also, there are n_B coordinates $\bar{q}_m$ that are to be eliminated in this process of creating a set of mass-additive coordinates consistent in size with the constrained system ma-

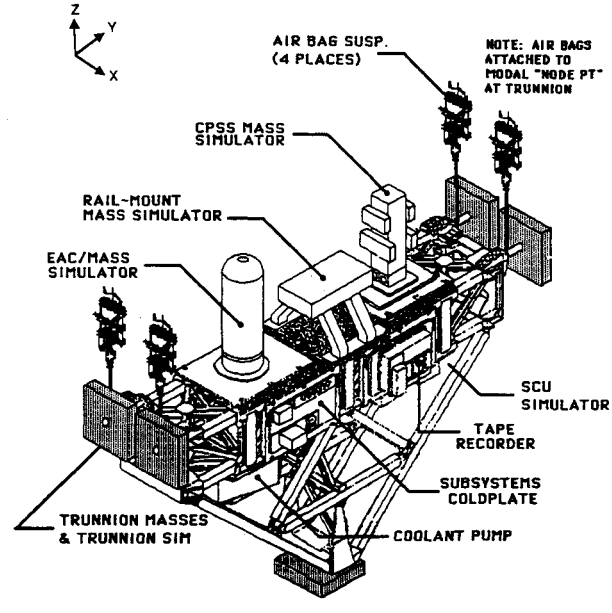

Fig. 2 Material Science Laboratory (MSL) payload in mass-additive test configuration.

trices. Columns of the mode shape matrix in Eq. (6) are partitioned in the manner shown to set up the conditions for constrained boundary degrees of freedom. The left columns correspond to the eliminated mass-additive coordinates, and the right columns correspond to the retained coordinates. It is noted that no mode shapes are eliminated, only generalized coordinates. Check cases for the procedures described in this section verified that the results were not significantly affected by the set of modes chosen for the left columns of Eq. (6) and corresponding to the eliminated coordinates. For convenience, the first consecutive n_B modes should be placed in the left column partition. Again, the full set of mass-additive coordinates cannot be used because the size of constrained system matrices is $n-n_B$.

To constrain the model, the boundary coordinates in Eq. (6) are set equal to zero, which allows the generalized coordinates to be written in the form

$$\begin{Bmatrix} \bar{q}_m \\ \hat{q}_m \end{Bmatrix} = \begin{Bmatrix} -[\bar{\Phi}_m^B]^{-1}[\hat{\Phi}_m^B] \\ I \end{Bmatrix} \{\hat{q}_m\} \tag{7}$$

or

$$\{q_m\} = [T_c]\{\hat{q}_m\} \tag{8}$$

Using Eq. (8) to transform the equations of motion for a model without boundary masses, Eq. (4), yields the constrained equations with unloaded boundaries in terms of the reduced set of mass-added modes,

$$[T_c]^T(I-[\Phi_m]^T[\Delta M][\Phi_m])[T_c]\{\ddot{\hat{q}}_m\}$$

$$+[T_c]^T[\omega_m^2][T_c]\{\hat{q}_m\} = [T_c]^T[\Phi_m]^T\{f(t)\} \tag{9}$$

Solution of Eq. (9) gives the natural frequencies and mode shapes in reduced mass-added modal coordinates $[\hat{\omega}^2]$ and $[\hat{\Phi}]$. Finally, the desired constrained modes in original coordinates are obtained by back-transformation,

$$[\bar{\Phi}_R] = [\Phi_m][T_c][\hat{\Phi}] \tag{10}$$

Equation (10) expresses the constrained mode shapes in terms of the measured (or retained analytical) free-free mass-additive modes.

By constraining the boundaries of the full updated analytical model, the exact fixed-base modes $[\Phi_R]$ are obtained. A cross-orthogonality check of the form

$$[\Phi_R]^T[M][\bar{\Phi}_R] \tag{11}$$

can be performed to determine the accuracy of the modes derived from mass-added vectors. It is noted that n_B rows of zeros must be added to the exact mode shape matrix to perform the multiplication with the $(N \times N)$ mass matrix. If the diagonal values of the cross-orthogonality matrix are between 0.9 and 1.0, the derived modes are considered to correlate well with the exact mode shapes. Comparison of exact and derived frequencies provides another measure of the accuracy of the method and is the primary check used in the following sections.

Demonstration of the Method for a Simple Beam

The method developed in the previous section is demonstrated analytically for a simple beam in Fig. 3. It can be seen that the technique involves the superposition of free-free mass-additive modes, subsequent transformation of the original unloaded model to express the equations of motion in mass-added coordinates, and constraint of the boundaries. The result is the desired set of fixed-base modes.

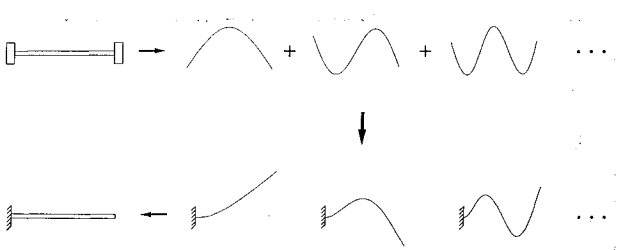

Fig. 3 Demonstration of mass-additive method for beam.

Results for a 1227-lb beam (4.5 × 8-in. cross section and 10-ft length) with 100-lb masses attached to the boundaries are shown in Table 1. The first 20 analytical mass-additive modes were used in Eqs. (9) and (10) to obtain the constrained analytical modes and frequencies. In Table 1, the exact and derived cantilever frequencies are shown with the cross correlation between the modes. Good convergence was obtained with a small number of mass-added modes for this simple case. The advantage of mass loading the boundaries to aid derivation of fixed-base modes and frequencies is illustrated in Table 2, where derived fixed-base frequencies are compared for an unloaded beam model and a mass-loaded model. For the unloaded model, the first 20 free-free modes were superposed, whereas for the mass-loaded model the first 20 mass-additive modes were used. In both cases the procedure described in the previous section was used to derive the modes. It is obvious that derived frequencies are more accurate for the model with mass added to the boundaries. The effect of mass loading becomes even more apparent for large complex structures, as will be seen next.

Application of Mass-Additive Technique to Space Shuttle Payloads

Material Science Laboratory

As stated earlier in the paper, free boundary mass-additive modal tests have been successfully performed for Space Shuttle payloads,[1,5,8] although the verification of constrained models using the test data was not adequately demonstrated previously. One such test[5] was performed for the payload shown in Fig. 2, the Material Science Laboratory (MSL). The payload in the test configuration had 400-lb trunnion masses and 800-lb keel mass. The four trunnion masses were rectangular, having dimensions of 25 × 20 × 3 in., and the keel mass was 27-in. square with 4-in. thickness. All masses were constructed of carbon steel. The payload weight was approximately 4450 lb, such that the ratio of added mass to structure mass was more than 50% for this case. Mass sizes for the test were initially chosen through the use of a finite element model to bring the trunnion and keel modes into the frequency range of the global modes.

After the MSL finite element model had been updated using the mass-additive test data,[9] constrained modes for seven boundary degrees of freedom (DOF) fixed were obtained by

Table 1 Comparison of exact and derived constrained frequencies for simple beam (20 mass-additive modes used)

Mode no.	Exact frequency	Derived frequency	Cross correlation
1	10.1988	10.2890	0.99999
2	63.9149	64.5479	0.99993
3	178.9635	180.9317	0.99967
4	350.6970	355.2167	0.99891
5	579.7276	587.2149	0.99739

Table 2 Comparison of derived constrained frequencies for simple beam with mass-loaded and unloaded boundaries (20 mass-additive and free-free modes)

Exact frequency	Derived frequencies	
	Mass loaded	Unloaded
10.1988	10.2890	11.1974
63.9149	64.5479	70.4302
178.9635	180.9317	197.9456
350.6970	355.2167	389.6016
579.7276	587.2149	647.3886

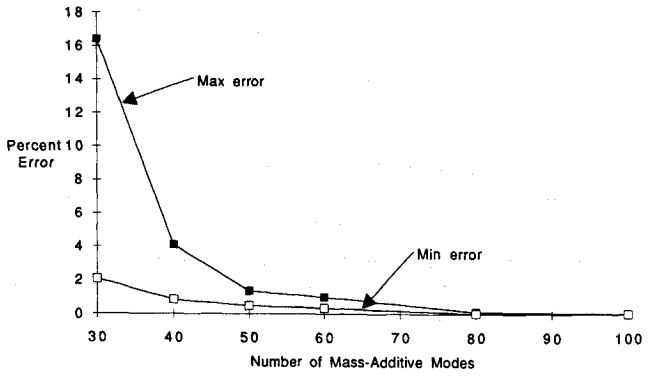

Fig. 4 Error between exact and derived constrained frequencies for MSL payload (based on first four constrained modes).

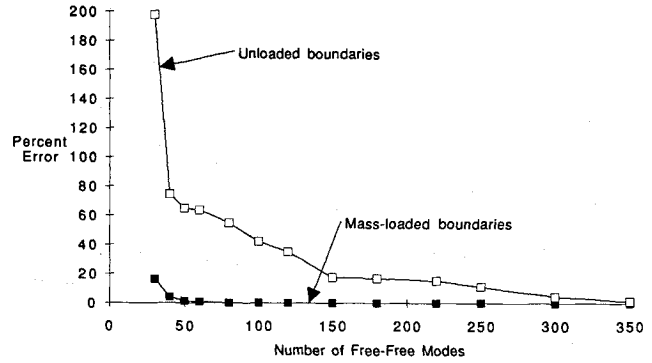

Fig. 5 Constrained frequency error comparison for MSL payload with mass loaded and unloaded boundaries.

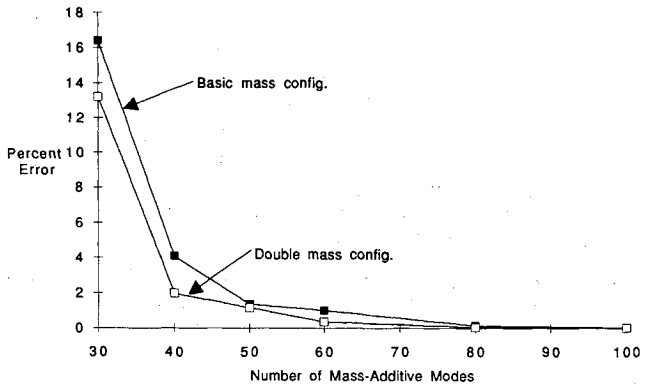

Fig. 6 Error reduction in constrained frequencies for MSL due to increased boundary mass.

eliminating the necessary DOF. However, accuracy of the derived constrained modes was not discussed in a quantitative manner in Ref. 9. This has been the approach taken in the past in practical application of the mass-additive technique due to an insufficient analytical methodology. The necessary methodology presented in this paper for quantifying the accuracy of derived constrained modes is applied in the following paragraphs.

The test-correlated MSL finite element model described in Ref. 9 was used two ways in the current study: 1) to compute "exact" constrained frequencies from the full model and 2) to compute "derived" constrained frequencies from a reduced model based on mass-added mode shapes [Eq. (9)]. In the first three columns of Table 3, comparison of constrained frequencies for the full updated model ("exact" case) and a mass-additive model with 40 retained modes ("derived" case) is shown for the test configuration. Studies were also performed using Eqs. (9–11) to determine the number of mass-additive modes required to derive fixed-base modes of sufficient accuracy. Figure 4 shows the error between exact and derived constrained frequencies as a function of the number of mass-additive modes used in the analysis. For a given number of mass-additive modes, the maximum and minimum errors encountered in deriving the first four fixed-base modes were calculated. It can be seen that, for the MSL configuration tested, at least 50 mass-added modes would have to be measured to derive fixed-base frequencies within 1% of the exact frequencies. This error limit was chosen to allow reasonable opportunity to achieve the 5% test/model frequency error requirement for Shuttle payloads. Figure 5 illustrates the benefit of mass loading the boundaries to derive constrained modes as opposed to using simple free-free modes with unloaded boundaries. The benefit is much more apparent for this complex structure than for the simple beam discussed previously.

Additional studies were done for the MSL payload to determine a mass configuration requiring fewer mass-additive test modes. It is noted that 30 mass-additive modes were measured in the MSL modal survey test.[5] Measurement of 50 modes as discussed in the previous paragraph would likely require a large increase in instrumentation for the test article. The effect of doubling the boundary masses, using 800 lb attached to each trunnion and 1600 lb on the keel, is shown in Fig. 6 and the fourth column of Table 3. It is seen in Fig. 6 that the error is reduced by 50% when using 40 mass-additive modes, although the overall improvement is not nearly as significant as might be expected. Further, it appears impractical to implement a test with masses of such size.

At this point it is appropriate to note that when a lumped mass is attached to the boundary of a test article, some DOF are loaded that should be left totally free. For example, in the MSL test all six boundary DOF at each trunnion and the keel were affected by the attached masses, when it was desirable that only one or two translational DOF be loaded for each attach point. To assess this effect of undesired inertia loading, a case was investigated for ideal point masses attached at the five constraint points for the MSL. Results are shown in Table 3, where the derived frequencies are compared with exact frequencies for the basic test configuration, the double mass configuration, and the ideal point mass case. It is apparent that convergence is much better for the ideal mass case compared with the other two configurations. These results indicate that the minimal improvement seen when the added masses are increased (Fig. 6) is likely due to undesired inertia loading.

The effect on convergence of the number of boundary DOF to be constrained is shown in Fig. 7. As expected, more mass-additive modes are required for highly redundant boundaries. Finally, several perturbations of the basic mass (test) configuration were investigated to determine the effect of loading some boundaries while leaving others unloaded. All of the studies for the MSL payload showed that a minimum of 40–50 free-free mass-additive modes must be measured to derive constrained modes of sufficient accuracy. Measurement of this many modes imposes difficulty, although it appears

Table 3 Comparison of exact and derived constrained frequencies for MSL payload (40 mass-additive modes used)

Mode no.	Exact frequency	Derived frequencies		
		Test configuration	Double mass	Ideal mass
1	13.6779	14.2359	13.9467	13.6941
2	18.7771	19.1085	18.9857	18.7971
3	21.3016	21.5578	21.5758	21.3111
4	29.0195	29.2683	29.5078	29.0745
5	30.5975	30.7340	30.7488	30.6107

possible if the test article were instrumented in sufficient detail, i.e., if a sufficient number of accelerometers were available.

Space Station Common Module Prototype

Applicability of the mass-additive technique was also investigated for the space station common module prototype (CMP) shown in Fig. 8 in a free-boundary mass-additive test configuration. The CMP is a cylinder 40 ft long by 14.5 ft in diameter that weighs approximately 7000 lb. As for the MSL payload, the number of mass-added modes required to derive sufficiently accurate constrained frequencies (1% error) was determined using a model correlated with test data. It can be seen in Fig. 9 that for the CMP, a complex shell structure, more mass-additive modes are required than for the trusslike MSL structure. Figure 9 shows that approximately 200 mass-added free-free test modes are required to derive fixed-base frequencies accurate to 1%. This result was not completely unexpected, since the CMP is a hollow structure characterized by high modal density and many local shell modes. It is expected that better results would be obtained for an actual module with internal structure intact.

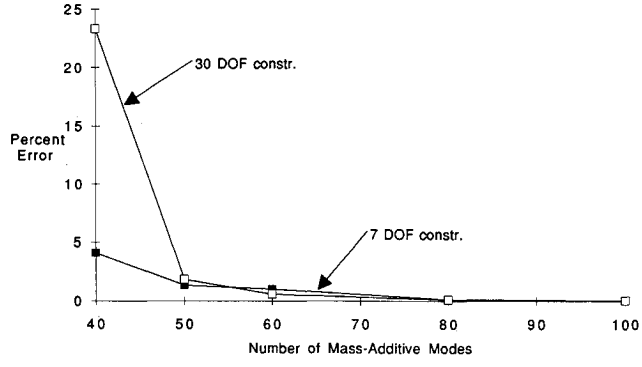

Fig. 7 Frequency error comparison for MSL payload with 7 and 30 boundary DOF constrained.

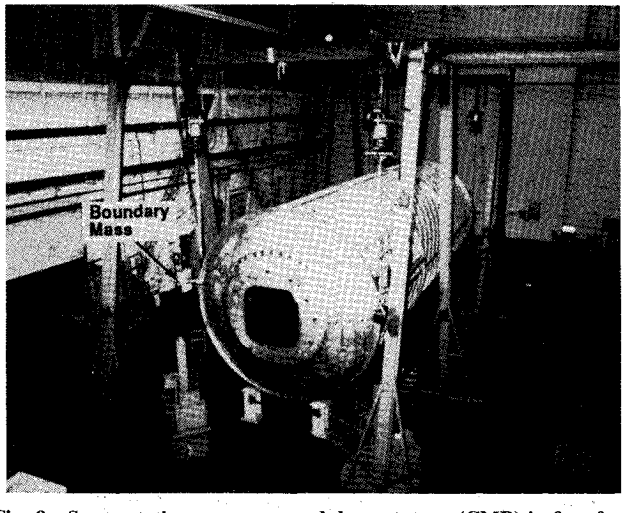

Fig. 8 Space station common module prototype (CMP) in free-free mass-additive test configuration.

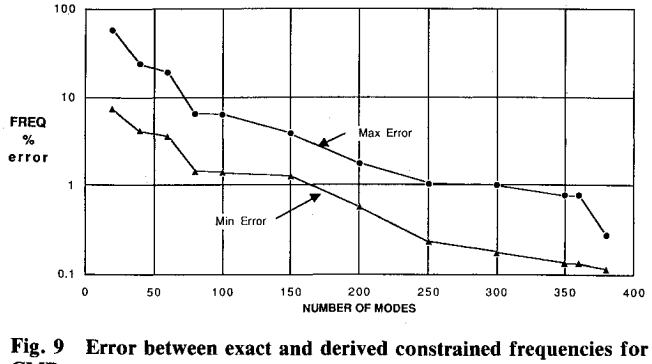

Fig. 9 Error between exact and derived constrained frequencies for CMP.

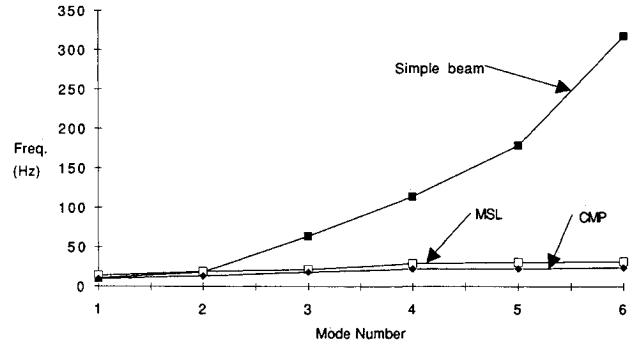

Fig. 10 Frequency as function of mode number for beam, MSL, and space station CMP.

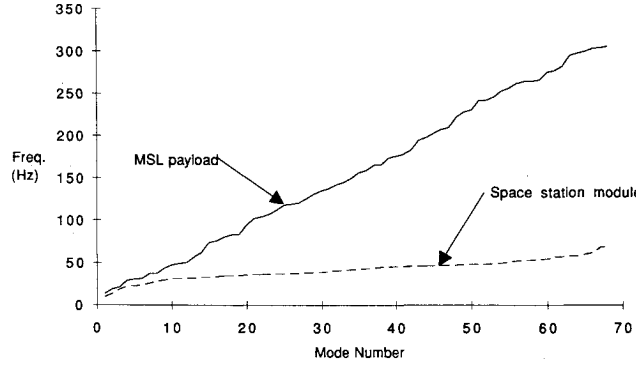

Fig. 11 Frequency as function of mode number for MSL and Space Station module payloads.

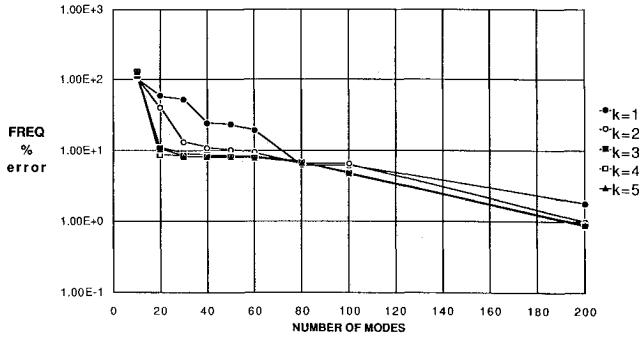

Fig. 12 Frequency error comparison for CMP with increased boundary mass.

In Fig. 10 a comparison of the fixed-base frequency distributions as functions of mode number is shown for the simple beam, MSL payload, and space station module. Although only a few modes are shown in Fig. 10, not providing great detail for the MSL and CMP, it does show the relative modal densities for the structures. Figure 11 provides more detail for the Shuttle payloads. In the three cases studied, it was found that, provided a sufficient number of test modes could be measured, the mass-additive technique worked well for continuous structures with well-spaced frequencies but not for a hollow shell-like structure with high modal density. Physically, this implies that, for the mass-additive method to be applicable, the stiffness characteristics of the interface support

Table 4 Constrained frequency and cross correlation comparisons for CMP payload (33 mass-additive modes)

Mode no.	Exact frequency	Mode no.	Derived frequency	Cross correlation
1	9.7913	1	12.5269	0.97980
2	13.3956	2	15.4446	0.96734
3	18.3037	3	19.4525	0.94983
4	22.3811	4	22.4337	0.99745
5	22.5663	5	22.6048	0.99942
6	23.7289	6	24.9709	0.95428
7	25.7756	7	28.5186	0.64167
8	28.4371	8	29.9701	0.92929
9	29.5605	7	28.5186	0.74574
10	31.2879	14	42.5608	0.10102

Table 5 Constrained frequency and cross correlation comparisons for CMP payload (80 mass-additive modes)

Mode no.	Exact frequency	Mode no.	Derived frequency	Cross correlation
1	9.7913	1	10.3919	0.99793
2	13.3956	2	14.2776	0.99559
3	18.3037	3	18.5679	0.99844
4	22.3811	4	22.4070	0.99984
5	22.5663	5	22.5891	0.99998
6	23.7289	6	24.3237	0.99680
7	25.7756	7	26.3608	0.99465
8	28.4371	8	28.5561	0.99960
9	29.5605	9	29.7559	0.99564
10	31.2879	10	31.3418	0.99502

regions must be such that significant flexure or exercising of the mass-loaded interfaces (trunnions and keel for the current example) is achieved. Each structure that is considered for a mass-additive test must be analyzed using the procedure developed in this paper, or a similar procedure, to assess the applicability of the technique.

Studies were also conducted for the CMP to determine if different mass configurations would decrease the number of test modes required to obtain the constrained modes. The test configuration had 200-lb masses attached to the four trunnions and the keel, and as for the MSL, the masses were initially sized to bring interface modes into the desired frequency range of the modal test. All five rectangular masses for the test configuration were constructed of steel, having dimensions of 12×20 in. with 3-in. thickness. As shown analytically in Fig. 12, increasing the added mass by factors of 2 through 5 (k in Fig. 12) does not provide enough improvement to make the method applicable for the CMP shell structure. Finally, a study was done in which the mass-added modes contributing most to the fixed-base modes were superposed to derive the constrained modes. Improvement was seen, and although this result is significant for other classes of structures, it is not sufficient for the space station module. Some other results of the CMP study are shown in Tables 4 and 5, where the "exact" constrained frequencies were obtained from the full updated analytical model and the "derived" frequencies from the mass-added model.

Summary

A procedure has been developed to derive constrained or fixed-base modes and frequencies using free-boundary mass-added modes along with analytical mass and stiffness matrices. The mass-added modes can either be measured and used directly in Eqs. (2–10), or analytically generated from a model that has been updated using measured mass-additive modes and frequencies. The latter approach was used for the Shuttle payloads described in the previous section. Problems associated with the design, construction, and checkout of fixed-base test fixtures can be avoided for structures to which the method is applicable. Accuracy of the derived modes and frequencies, as well as the applicability of the method for a particular structure, can be assessed using the methodology presented in this paper. Results obtained for a simple beam and two classes of Shuttle payloads yielded several observations.

1) Superposition of free-boundary normal modes to obtain constrained modes converges much more quickly when the boundaries are mass loaded.

2) The method worked much better for continuous structures with well-spaced frequencies than for a hollow shell-like structure having high modal density. Each structure considered for a mass-additive test must be analyzed for applicability of the method.

3) The improvement obtained by increasing the added mass or perturbing the mass configuration is minimal, likely due to undesired inertia loading; i.e., attached masses affect some DOF that should be left completely free.

4) Derivation of constrained modes generally requires a large number of mass-additive test modes. This appears achievable but imposes some difficulty in testing.

5) Sizing of masses is not completely arbitrary. General size required is governed by frequency bandwidth for global modes, whereas more precise design is aided using the methodology developed in this paper.

References

[1]Coleman, A. D., Anderson, J. B., Driskill, T. C., and Brown, D. L., "A Mass Additive Technique for Modal Testing as Applied to the Space Shuttle ASTRO-1 Payload," *Proceedings of the 6th International Modal Analysis Conference,* Society for Experimental Mechanics, Bethel, CT, 1988, pp. 154–159.

[2]Goldenberg, S., and Shapiro, M., "A Study of Modal Coupling Procedures for the Space Shuttle," NASA CR-112252, April 1973.

[3]Gwinn, K. W., Lauffer, J. P., and Miller, A. K., "Component Mode Synthesis Using Experimental Modes Enhanced by Mass Loading," *Proceedings of the 6th International Modal Analysis Conference,* Society for Experimental Mechanics, Bethel, CT, 1988, pp. 1088–1093.

[4]Baker, M., "Component Mode Synthesis Methods for Test-Based, Rigidly Connected, Flexible Components," AIAA Paper 84-0943, May 1984.

[5]Kinney, T. L., "Material Science Laboratory (MSL) Carrier Modal Survey Test Summary and Model Correlation," Teledyne Brown Engineering, PMIC-RPT-6925, Huntsville, AL, June 1990.

[6]Anon., "The Fundamentals of Modal Testing," Hewlett-Packard Co., Application Note 243-3, Palo Alto, CA, May 1986.

[7]Benfield, W. A., and Hruda, R. F., "Vibration Analysis of Structures by Component Mode Substitution," *AIAA Journal,* Vol. 9, No. 7, 1971, pp. 1255–1261.

[8]Chandler, K. O., Driskill, T. C., and Lindner, J. L., "Space Station Module Free-Free Modal Survey Test Report," NASA Marshall Space Flight Center, SS-DEV-ED90-061, Huntsville, AL, Oct. 1990.

[9]Kinney, T. L., "Material Science Laboratory (MSL) Carrier Nastran Model Description," Teledyne Brown Engineering, PMIC-RPT-6924, Huntsville, AL, June 1990.